Journal of Solid State Chemistry 182 (2009) 799–806

Contents lists available at ScienceDirect

Journal of Solid State Chemistry

journal homepage: www.elsevier.com/locate/jssc

Structural features, nonstoichiometry and high-temperature transport in $SrFe_{1-x}Mo_xO_{3-\delta}$

A.A. Markov [a], O.A. Savinskaya [b], M.V. Patrakeev [a,*], A.P. Nemudry [b], I.A. Leonidov [a], Yu.T. Pavlyukhin [b], A.V. Ishchenko [c], V.L. Kozhevnikov [a]

[a] Institute of Solid State Chemistry, UB RAS, 91 Pervomaiskaya Str., 620219 Ekaterinburg, Russia
[b] Institute of Solid State Chemistry and Mechanochemistry, SB RAS, 18 Kutateladze Str., 630128 Novosibirsk, Russia
[c] Boreskov Institute of Catalysis, SB RAS, 5 Lavrentiev Ave., 630090 Novosibirsk, Russia

ARTICLE INFO

Article history:
Received 9 October 2008
Received in revised form
24 December 2008
Accepted 31 December 2008
Available online 6 January 2009

Keywords:
Strontium ferrite
Mixed conductivity
Perovskite
Brownmillerite
Oxygen nonstoichiometry
Ion conductivity
Electron mobility

ABSTRACT

The oxide solid solutions $SrFe_{1-x}Mo_xO_{3-\delta}$, where $x = 0.05$, 0.1 and 0.2, are studied in this work. It is shown that substitution of iron for molybdenum results in stabilization of a cubic quasi-perovskite locally inhomogeneous structure, which is evidenced by HREM and Mössbauer spectroscopy. The coulometric titration is used in order to determine changes of oxygen nonstoichiometry in the obtained solutions with temperature and ambient oxygen partial pressure. Partial molar thermodynamic functions of the labile oxygen are calculated from the measured data. The variations of partial molar entropy with oxygen content follow the ideal gas model reasonably well thus demonstrating approximately random distribution of oxygen vacancies in the doped ferrite at high temperatures. The partial molar enthalpy is found to increase with doping, which is indicative of a progressive decrease in average values of the bonding energy of labile oxygen ions. The measurements of total conductivity are used in order to determine partial contributions of charge carriers. The oxygen ion component is shown to increase at small level of doping, $x = 0.05$ while further increase in molybdenum content is accompanied with the decline in the ion conductivity. The electron contribution in reducing conditions tends to increase with molybdenum content, which is interpreted as a manifestation of involvement of Mo^{5+} cations in electron transport. Concentration and mobility of electron carriers are calculated. Some increase in mobility of electron holes at small doping is explained as related to the filling of oxygen vacancies.

1. Introduction

The strontium ferrite $SrFeO_{3-\delta}$ is known to exhibit fast oxygen-ion transport and appreciable electron conductivity at moderately high temperatures [1,2]. These properties combination is attractive for the use of $SrFeO_{3-\delta}$ as a base for development of SOFC electrodes and oxygen separating membranes [3–6]. Depending on the nonstoichiometry value, δ, the ferrite may crystallize with several modifications that differ in the distribution of oxygen vacancies over crystalline lattice [7]. The distribution of vacancies impacts considerably the ion and electron transport, and is governed mainly by the interplay of coulomb repulsion and heat movement energies. For instance, at temperatures below 900 °C the most stable form of the ferrite with maximal nonstoichiometry $\delta = 0.5$ is a brownmillerite-type phase $Sr_2Fe_2O_5$ [8] where oxygen vacancy long-range ordering results in regular alternation of layers of oxygen–iron octahedra and tetrahedra [9]. Generally, the ordering is regarded as undesirable because it leads to the removal of the vacancies from oxygen transfer and to deterioration of transport characteristics. However, the long-range ordering is not the only means for the vacancies to reduce their free energy in the crystalline lattice. Thus, authors [10–12] have shown that lattice relaxation in perovskite-like oxides can occur also via formation of multiple, spatially randomly oriented but locally ordered domains where considerable part is clustered of all vacancies in the oxide. The typical size of the vacancy ordered domains is smaller than the coherence length for X-ray scattering [13]. Therefore, the diffraction pattern for such a peculiar nanostructure can often look like corresponding to symmetry higher than, in fact, it is on microscopic scale. In difference with long-range ordering type, the presence of highly developed domain boundaries where vacancy ordering is not perfect (and, in addition, of some amount of randomized vacancies left outside the domains) can favor rather substantial oxygen transport [13]. In particular, this structural architecture is believed to be the reason for large ion conductivity (0.2 S/cm at 900 °C) in the high-temperature cubic quasi-perovskite phase $SrFeO_{3-\delta}$, where $\delta = 0.45/0.50$ [14]. The stabilization of this favorable structural

* Corresponding author. Fax: +7 343 3744495.
E-mail address: patrakeev@ihim.uran.ru (M.V. Patrakeev).

0022-4596/$ - see front matter © 2009 Elsevier Inc. All rights reserved.
doi:10.1016/j.jssc.2008.12.026

state within wider limits of temperature can be achieved by B-site doping as demonstrated in works [15–18] where transport properties are studied at partial replacement of iron for Ti, Ga, Al and Sc. Recently, authors [19] have found that up to 50% of iron in $SrFeO_{3-\delta}$ can be replaced for molybdenum. It is known that molybdenum tends to have higher oxidation state than iron. Therefore, this substitution should increase the oxygen content in $SrFeO_{3-\delta}$ and the average coordination of iron by oxygen, and, consequently, one can await some decrease in the average size of the vacancy ordered domains, i.e., enhanced nano-structuring in the doped ferrite. Further still, these effects are expected to take place at comparatively small concentration of the dopant because of the appreciable difference in the formal charges of molybdenum and iron cations. If that is the case, the perturbation in the crystalline lattice of the ferrite, as caused by the doping, is not anticipated to be so strong as to influence deleteriously upon transport properties. With these arguments in mind, we studied specimens $SrFe_{1-x}Mo_xO_{3-\delta}$, where $x = 0.05$, 0.1 and 0.2, with the aim to find out how molybdenum substitution may influence structure, stability, oxygen thermodynamics and transport properties in the strontium ferrite.

2. Experimental

In present work were employed samples $SrFe_{1-x}Mo_xO_{3-\delta}$, where $x = 0.05$, 0.1 and 0.2, synthesized earlier; X-ray spectra and crystal lattice parameters can be found in Refs. [19,20]. Additional characterization of the selected specimens were carried out by means of Mössbauer spectroscopy and high-resolution electron microscopy (HREM). A number of reduced samples were obtained by quenching to room temperature after equilibration at 950 °C and $pO_2 = 10^{-4}$ atm. Rectangular slabs $2 \times 2 \times 15$ mm cut from the sintered pellets were utilized for the four-probe d.c. conductivity measurements that were carried out with the help of a special cell made of zirconia oxygen-ion electrolyte. One pair of platinum electrodes deposited upon the cell served in order to vary and maintain oxygen partial pressure, pO_2, while the other one was used as an oxygen sensor for independent control of the oxygen partial pressure inside the cell. The temperature of the experiment was set with the help of the external furnace. The changes of equilibrium oxygen content in the specimens with temperature and oxygen partial pressure were measured by making use of a coulometric titration technique based also on exploitation of the sensing and pumping properties of solid oxygen electrolytes. Further experimental details can be found elsewhere [21,22].

3. Results and discussion

The coulometric titration results are shown in Fig. 1. The literature data [19] suggest that oxygen removal from $SrFe_{1-x}Mo_xO_{3-\delta}$ at heating and/or oxygen pressure decrease results in reduction of iron, $Fe^{4+} \rightarrow Fe^{3+}$, while molybdenum cations maintain their oxidation state 6+. Therefore, oxygen content within 650–950 °C and 10^{-8}–10^{-12} atm, where inflexion of the titration curves can be observed (middle-pressure range), is determined by the ratio of Fe^{3+} and Mo^{6+} cations. Correspondingly, the charge balanced formula of the doped ferrite in these conditions can be represented as $Sr^{2+}Fe^{3+}_{1-x}Mo^{6+}_{x}O^{2-}_{3-(0.5-1.5x)}$. At pressure increase, right to the inflexion vicinity (high-pressure range), oxygen intercalation into the structure takes place with formation of Fe^{4+}, i.e. electron holes localized on Fe^{3+} cations

$$2Fe^{3+} + V_O + \frac{1}{2}O_2 \leftrightarrow 2Fe^{4+} + O^{2-} \quad (1)$$

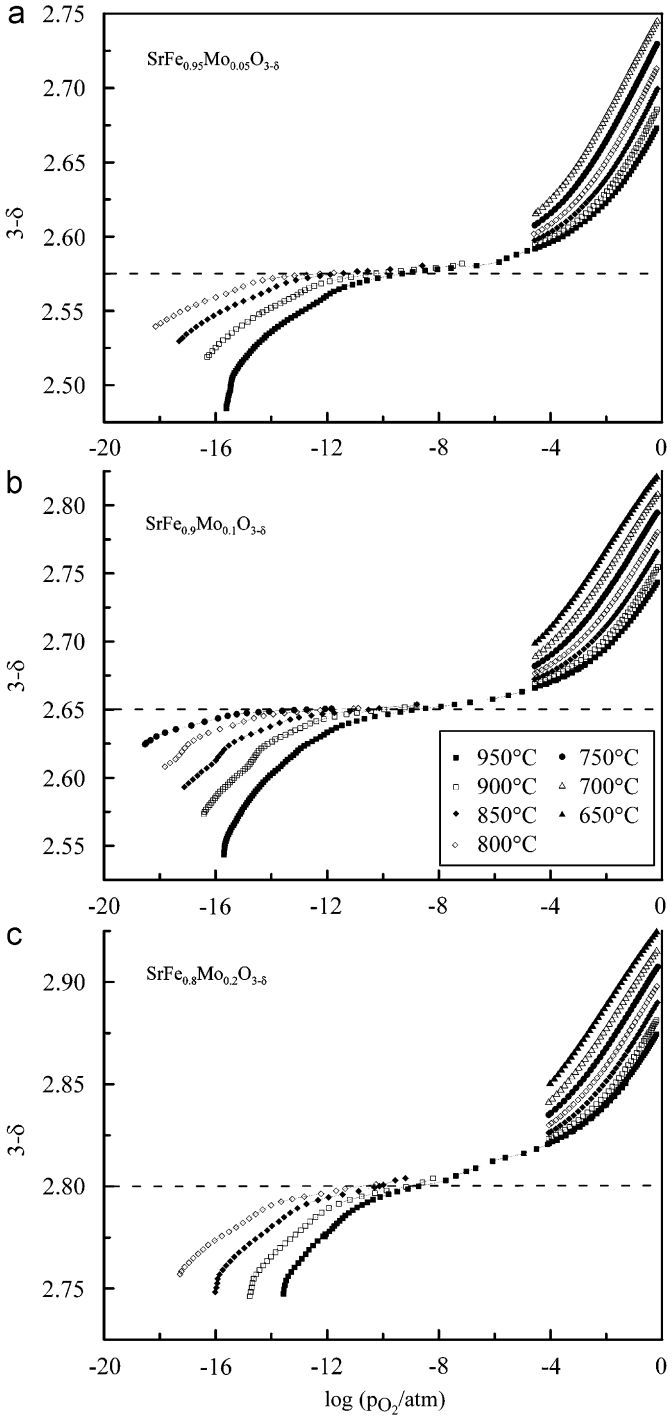

Fig. 1. The coulometric titration data for $SrFe_{1-x}Mo_xO_{3-\delta}$, where $x = 0.05$, 0.1 and 0.2. The dashed line corresponds to the oxygen concentration in the samples containing iron in 3+ and molybdenum in 6+ oxidation states only.

The pressure decrease, left to the inflexion vicinity (low-pressure range), results in oxygen depletion from the crystalline lattice. In this extreme of rather small oxygen pressure values one can expect partial reduction of both iron and molybdenum with formation of Fe^{2+} and Mo^{5+} cations, i.e. electrons localized on Fe^{3+} and Mo^{6+}

$$2Fe^{3+} + O^{2-} \leftrightarrow 2Fe^{2+} + V_O + \frac{1}{2}O_2 \quad (2)$$

$$2Mo^{6+}+O^{2-} \leftrightarrow 2Mo^{5+}+V_O+\frac{1}{2}O_2 \quad (3)$$

The data in Fig. 1 demonstrate also that the in-take of oxygen in the high-pressure range occurs less pronounced while depletion in the low-pressure range becomes easier in the specimens with larger amount of molybdenum. This gives clear evidence to the decrease in the average bonding energy of labile oxygen with the increase in doping. In order to gain better understanding of how molybdenum substitution may influence labile oxygen ions it is useful to track changes in partial molar thermodynamic functions of oxygen in the solid solutions. Experimental data in Fig. 1 enable one to calculate oxygen chemical potential in the ferrite relative to standard state in the gas phase as

$$\Delta\mu_O(\delta,T)=\frac{1}{2}RT\ln(pO_2) \quad (4)$$

where R and T designate the gas constant and absolute temperature, respectively. On the other hand, $\Delta\mu_O(\delta,T)$ is related with partial molar enthalpy, $\Delta\bar{H}_O(\delta)$, and entropy, $\Delta\bar{S}_O(\delta)$, of oxygen via known relation

$$\Delta\mu_O(\delta,T)=\Delta\bar{H}_O(\delta)-T\Delta\bar{S}_O(\delta) \quad (5)$$

The dependencies $\Delta\mu_O(\delta,T)$ at different δ's, indeed, change linearly with temperature. The respective fittings of the data from the high-pressure range result in partial molar thermodynamic functions in Fig. 2. Similar data for $SrFeO_{3-\delta}$ [23] are also shown for comparison. Except for the singular behavior in $SrFeO_{3-\delta}$ at $\delta\rightarrow 0.5$, which is caused by the structural transition [8], one can observe that the oxygen content increase is accompanied with some increase in $\Delta\bar{H}_O(\delta)$ values. This behavior is indicative of the repulsive interaction of labile oxygen ions in $SrFe_{1-x}Mo_xO_{3-\delta}$. The enthalpy values obtained from the low-pressure range data in Fig. 1 exhibit systematic increase from approximately −380 to −330 kJ/mol, as shown in the insert of Fig. 2b, and, thus, give additional confirmation to the decrease in the average bonding energy of labile oxygen with the increase in molybdenum content Table 1.

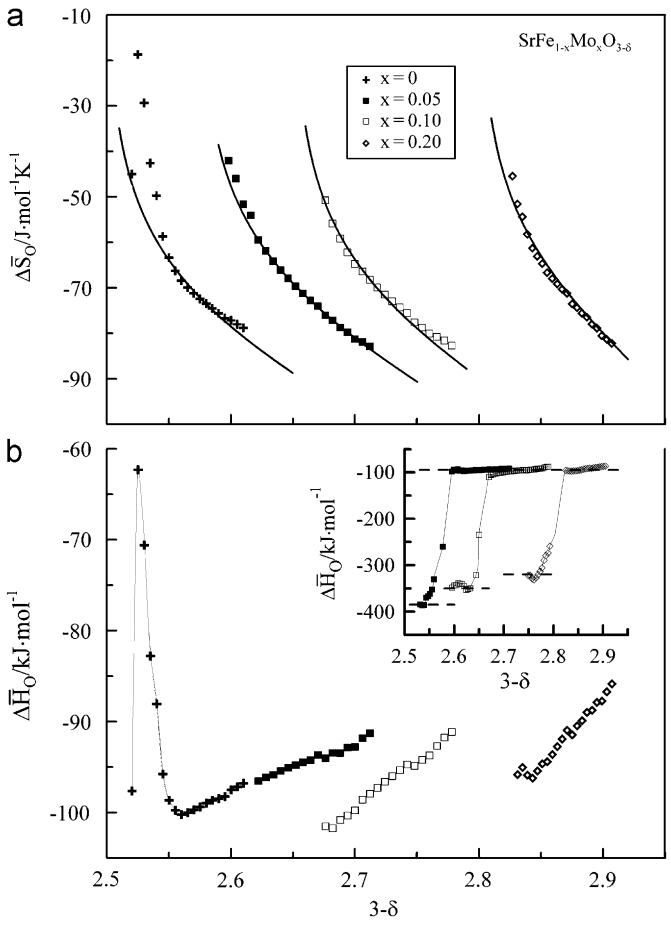

Fig. 2. The plots for partial molar: (a) entropy and (b) enthalpy of the labile oxygen in $SrFe_{1-x}Mo_xO_{3-\delta}$ as obtained from the data at $pO_2>10^{-5}$ atm in Fig. 1. Solid lines show results calculated according to Eq. (7). The insert in plot (b) exhibits partial molar enthalpy in the entire studied range of oxygen content.

Table 1
The activation energies and enthalpies in $SrFe_{1-x}Mo_xO_{3-\delta}$.

x	$\Delta\bar{H}_O$ (eV)	E_i (eV)	E_n (eV)	$E_{\mu p}$ (eV)	ΔH_{red} (eV)
0		0.3	2.2	0.3	
0.05	−3.9	0.6	2.1	0.2	3.7
0.1	−3.6	0.7	2.0	0.2	3.5
0.2	−3.3		1.9	0.2	3.3

The oxygen concentration changes of entropy, as can be seen in Fig. 2a, suggest some similarity in distribution of labile oxygen ions (and vacancies) over available positions in specimens with different x's. As a rough approach one can make an attempt to approximate the experimental data with the configuration part of entropy for reaction (1)

$$\Delta\bar{S}_O=R\ln\left(\frac{[V_O][Fe^{3+}]^2}{[O^{2-}][Fe^{4+}]^2}\right)+\text{const} \quad (6)$$

Taking into view that $[V_O]=\delta$, $[O^{2-}]=3-\delta$, $[Fe^{3+}]=2x+2\delta$, $[Fe^{4+}]=1-3x-2\delta$, this relation can be represented as

$$\Delta\bar{S}_O=R\ln\left(\frac{\delta(2x+2\delta)^2}{(3-\delta)(1-3x-2\delta)^2}\right)+\text{const} \quad (7)$$

The fitting results of experimental data with (7) are shown in Fig. 2a with solid lines. One can see that calculated plots and experimental points coincide fairly well. As it is said before, complicated behavior of thermodynamic functions in $SrFeO_{3-\delta}$ at extreme exhaustion of the labile oxygen is related to phase transition. Strong suppression of similar features in the plots for $\Delta\bar{H}_O(\delta)$ and $\Delta\bar{S}_O(\delta)$ in molybdenum substituted ferrites may be interpreted as evidence to efficient hindering of the vacancy ordering by doping. This conclusion is corroborated by X-ray data [20] that show formation of a cubic structure in the doped samples $SrFe_{1-x}Mo_xO_{3-\delta}$ after heat treatment in vacuum. Notice, that doubling of the perovskite lattice parameter, $a\approx 2a_p$, is peculiar for the reduced sample $x=0.05$. Similar structure for $SrFe_{1-x}V_xO_{2.5+x}$ was observed earlier in work [24]. It is shown that oxygen disordering develops with the increase in vanadium content as a result of micro-twinning and off-orientation of brownmillerite domains in six possible $\langle 110\rangle_p$ directions with simultaneous decrease in their average size. Though apparently cubic according to X-ray diffraction, $SrFe_{0.95}V_{0.05}O_{2.55}$ produced distinct super-structure spots on electron diffraction photographs that were interpreted as manifestation of brownmillerite domains with the size of 5–20 nm. When doping increases the domains degenerate into even smaller clusters where some vestigial ordering of oxygen vacancies persists only in the immediate vicinity of iron. Mössbauer spectroscopy of the quenched samples gives about the same picture of disordering in $SrFe_{1-x}Mo_xO_{3-\delta}$, as shown in Fig. 3 and Table 2. The spectra for $x=0$ and 0.05 can be described as a superposition of two Zeeman sestets characteristic of Fe^{3+} cations in octahedral and tetrahedral oxygen environment. The sestets merge at further increase in molybdenum content, $x\geqslant 0.1$, so that absorption lines acquire considerable broadening and asymmetry. These changes

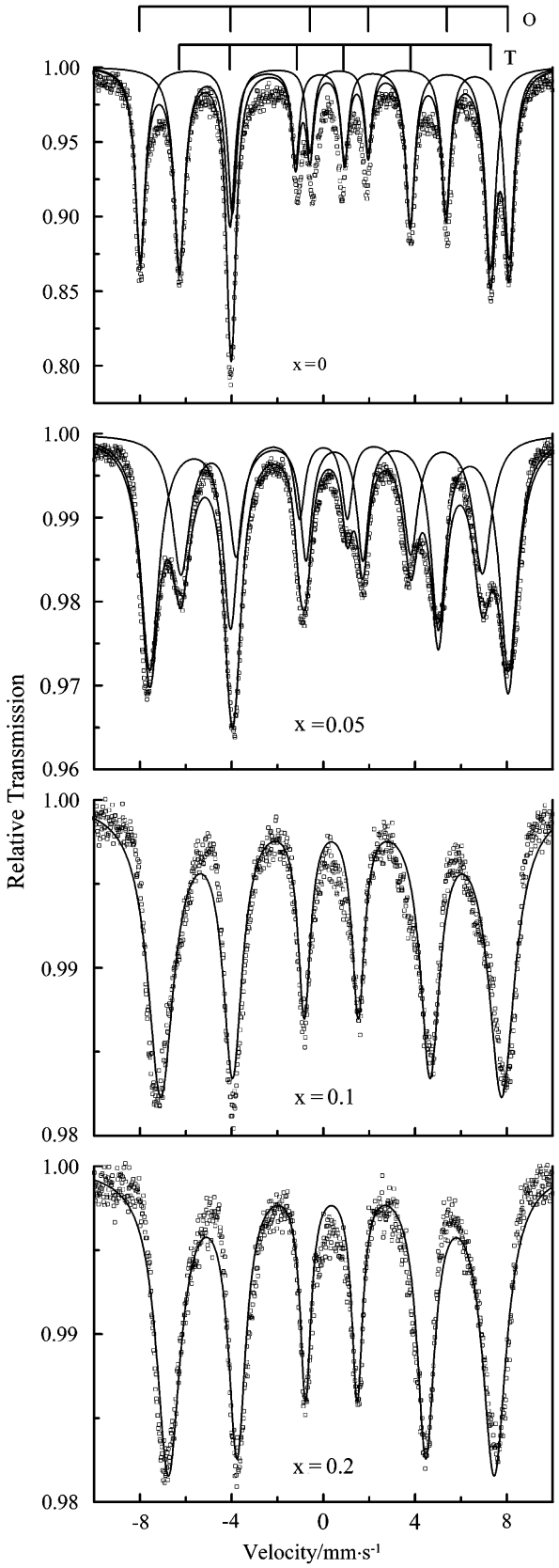

Fig. 3. The Mössbauer spectra for the quenched samples $SrFe_{1-x}Mo_xO_{3-\delta}$, where $x = 0$, 0.05, 0.1 and 0.2.

clearly confirm strong disordering in oxygen sub-lattice where iron cations with different oxygen environment occur intermingled. One more illustration of the microstructure in the reduced compound with $x = 0.05$ is obtained with the help of HREM, as shown in Fig. 4. One can observe nano-sized regions that bear distinct features of the local order different from the state in the surrounding crystal lattice. It ought to be noticed here that the rather straightforward results on local inhomogeneities are obtained with quenched specimens at room temperature, and, therefore, they do not imply any controversy with indirect results of thermodynamic equilibrium analysis that suggests less developed domains and more perfectly randomized oxygen sub-lattice in the doped samples at high-temperature. On the whole, molybdenum doping is a very effective means in order to randomize the oxygen sub-lattice in strontium ferrite. The minimal concentration of the dopant, which is necessary to retain apparently cubic structure in the ferrite at wide variations of oxygen content, is nearly 5%. This level of the doping favors a peculiar nano-structured state in the crystal lattice, which seems to persist at wide variations of oxygen content and temperature. The doping increase results in further suppression of local vacancy clusters and in the approach to perfectly homogeneous distribution of oxygen vacancies over crystalline lattice.

Table 2
Mössbauer parameters for samples $SrFe_{1-x}Mo_xO_z$ (quenched in reducing conditions).

x	N	Iron state	IS (mm/s)	QS (mm/s)	FWHM (mm/s)	B (T)	I (%)
0	1	Fe^{3+} (O)	0.40	1.20		47.49	52
	2	Fe^{3+} (T)	0.20	−1.35		39.92	48
0.05	1	Fe^{3+} (O)	0.37	−0. 12	0.55	48.76	63
	2	Fe^{3+} (T)	0.18	0.18	0.47	40.97	37
0.1	1	Fe^{3+} (O)	0.34	−0.002	0.53	46.33	
0.2	1	Fe^{3+} (O)	0.35	−0.002	1.46	44.31	

IS is the isomer shift relative to metallic α-Fe at 295 K.
QS, B are the quadrapole splitting and magnetic hyperline field, respectively.

The experimental conductivity, σ, isotherms are shown vs. oxygen partial pressure in Fig. 5. The results within 10^{-8} atm $< pO_2 < 10^{-4}$ atm are taken away from the picture because of the very sluggish kinetics of oxygen equilibration at these pressures that renders the data unreliable [25]. The conductivity is temperature activated at low pressures, $pO_2 < 10^{-8}$ atm. The characteristic minima on the isotherms correspond to the intrinsic electron n–p equilibrium [26]. It is important to see that the minima are located in the range of quite small pressures of oxygen (activities of oxygen, in strict terms) where variations of the pressure may bring about only so small changes in oxygen stoichiometry that they can be safely disregarded compared to the total oxygen content in the oxide. In these conditions the concentrations of n- and p-type carriers change with pressure as $pO_2^{-1/4}$ and $pO_2^{+1/4}$ near the minima [26]. Assuming pressure independent oxygen ion contribution, σ_i, the total conductivity can be approximated as

$$\sigma(T, pO_2)\sigma_i(T) + \sigma_n^o(T) \cdot pO_2^{-1/4} + \sigma_p^o(T) \cdot pO_2^{+1/4} \quad (8)$$

where coefficients $\sigma_n^o(T)$ and $\sigma_p^o(T)$ correspond to n- and p-conductivity level, respectively, at $pO_2 = 1$ atm. The nonlinear fittings with this expression approximate the experimental data quite satisfactorily, as shown in Fig. 5 (solid lines), thus giving confirmation to the correct using of relation (8). The errors in calculated values of $\sigma_i(T)$, $\sigma_n^o(T)$ and $\sigma_p^o(T)$ are estimated to be about 3%, 2% and 6%, respectively. In the case of the oxide with

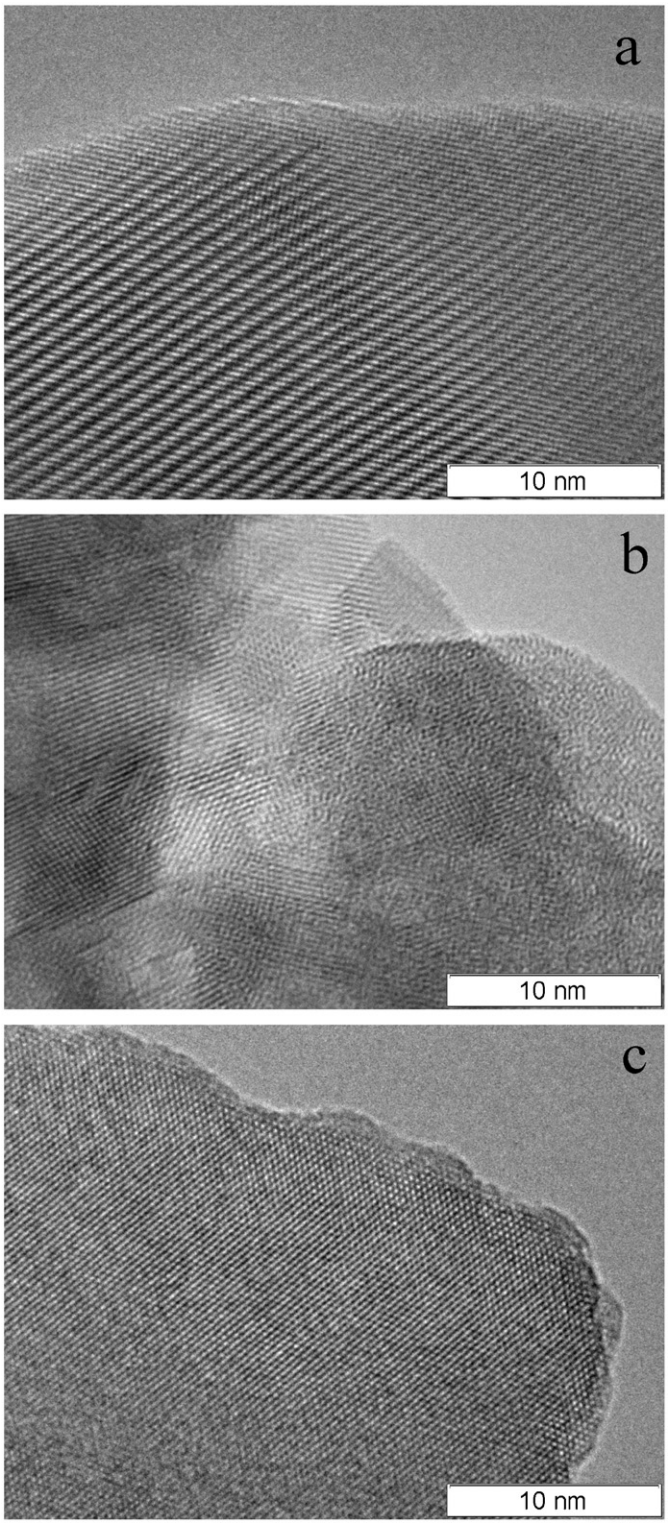

Fig. 4. HREM image for the quenched samples $SrFe_{1-x}Mo_xO_{3-\delta}$; with: (a) $x = 0$, (b) 0.05 and (c) 0.1.

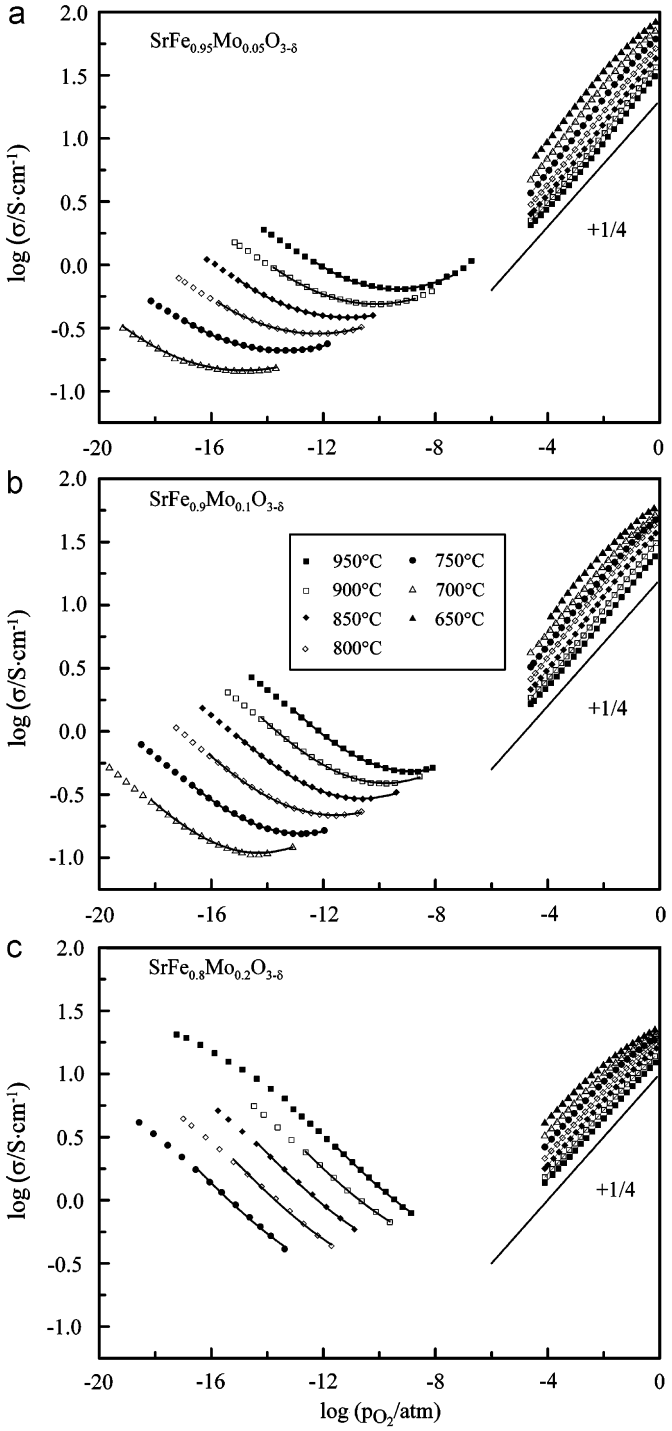

Fig. 5. The measured isotherms of conductivity vs. partial pressure of oxygen. The fitting results according to Eq. (8) are shown with solid lines.

$x = 0.2$, limited experimental data enable only calculation of σ_n^o with acceptable accuracy. The obtained ion conductivity is shown with Arrhenius coordinates in Fig. 6 together with the earlier data for $SrFeO_{3-\delta}$ [14]. It is seen clearly that even the minimal doping, $x = 0.05$, results in disappearance of the cusp related to the transition from brownmillerite to cubic quasi-perovskite structure, while the ion conductivity level in this sample unusually occurs even higher than in the parent ferrite. Ordinarily, the doping is accompanied with the ion conductivity decrease. One may suggest that in difference with the dopant in a smaller formal oxidation state, e.g. gallium or aluminum [17], the compensation of excessive positive charge at the introduction of higher charged Mo^{6+} cations into ferrite structure takes place as a result of the filling of oxygen vacancies not only in the immediate surrounding of the dopant but at a larger distance also thus giving way to formation of pseudo-interstitial oxygen ions. The more remote location results in a smaller oxygen bonding energy, as shown in

Fig. 2b, and in more efficient involvement of the oxygen ions in the transport. This mechanism is considered for oxygen conductor Ba_3InZrO_8 in work [27].

The electron, n- and p-type conductivity can be obtained by subtracting oxygen ion contribution from the total conductivity.

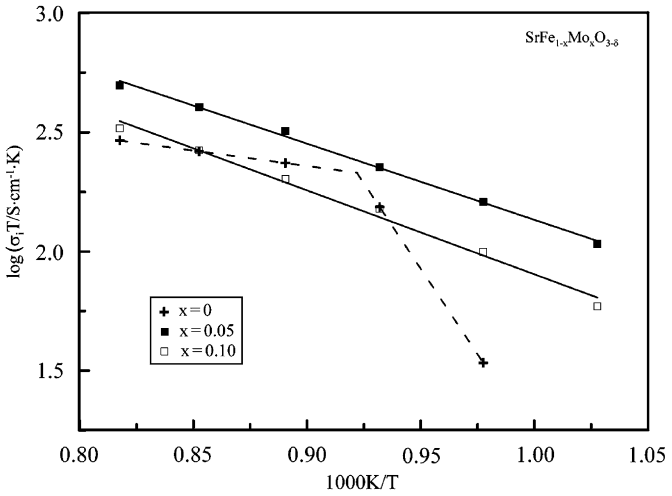

Fig. 6. Arrhenius plots for oxygen ion conductivity in $SrFe_{1-x}Mo_xO_{3-\delta}$.

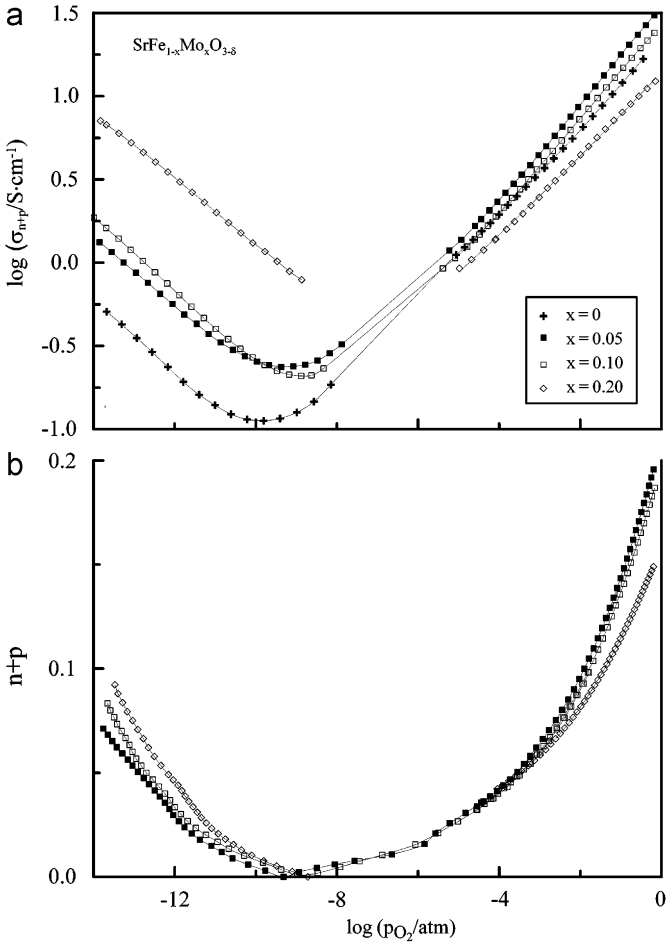

Fig. 7. (a) The isotherms of electron conductivity and (b) of total concentration per formula unit of p- and n-type charge carriers in $SrFe_{1-x}Mo_xO_{3-\delta}$ vs. partial pressure of oxygen.

As an example, results at 950 °C are shown in Fig. 7a. Considerable increase with doping can be observed for n-type electron contribution. For instance, it is an order of magnitude larger in oxide with $x = 0.2$ than in the parent ferrite $SrFeO_{3-\delta}$. In some part it may be again explained as reflecting some decrease in oxygen bonding energy that entails shift of reactions (2) and (3) to the right hand side and respective increase in concentration of electrons. This, however, cannot be a sole reason. Indeed, the concentration of n-type carriers can be calculated immediately from oxygen content data in Fig. 1, and it is not difficult to find out the concentration increase by a factor of one and a half at 950 °C with the change of x from 0.05 to 0.20, as can be seen in Fig. 7b. At the same time, the n-type conductivity becomes about six times larger, as shown in Fig. 7a. Hence, molybdenum doping favors the mobility increase. Combining conductivity and oxygen content data, rather straightforward calculations of mobility can be done with the using of expression

$$\mu_n = \frac{\sigma_n}{e \cdot n \cdot N} \tag{9}$$

Here, σ_n is n-type electron conductivity, e is elementary charge, $n = (3x+2\delta-1)$ equals the number of electrons per formula unit, and N is the number of formula units per unit volume that can be calculated from structural data. In order to minimize the contribution from electron holes the data in Fig. 7 at as low pressures as possible are utilized in calculations. Respective results are presented in Fig. 8. It is seen that n-type mobility in oxide with $x = 0.2$ is about five times larger than in $x = 0.05$. Such a change seems somewhat unusual because doping is connected with static disordering of transport chains "…metal–oxygen–metal…" and deterioration of both, n- and p-, electron conductivity types. In the present case, however, strong hybridization should be taken into account of iron and molybdenum t_{2g} states near the Fermi level [28] that favors electron transfer. The data in Fig. 8 can be used for estimation of the electron mobility activation energy, $E_{\mu n}$, which is found equal to 0.25 ± 0.05 eV. The apparent activation energy for electron conductivity, E_n, at permanent partial pressure of oxygen was evaluated from respective Arrhenius plots at $pO_2 = 10^{-14}$ atm, Table 1. This parameter tends to decrease with the increase in molybdenum content. Since the apparent activation energy for electron conductivity at a fixed pressure of oxygen consists from the energy necessary for formation of the carriers and the energy necessary for their transfer then the expression

$$E_n = \frac{\Delta H_{red}}{2} + E_{\mu n} \tag{10}$$

can be employed in order to evaluate the reduction enthalpy, ΔH_{red}, Table 1. It follows from the obtained data that the doping increase favors the enthalpy decrease, i.e. again the confirmation is made of the labile oxygen bonding energy decrease with replacement of iron for molybdenum. The consistency of the results is seen from a very good coincidence with the enthalpy data from thermodynamic calculations. It is important to stress here that enhanced oxygen lability is not accompanied with deterioration of thermodynamic stability of the doped samples. For instance, phase decomposition of $SrFeO_{3-\delta}$ at 950 °C occurs at $pO_2 = 3 \times 10^{-17}$ atm that can easily be detected in electrical conductivity measurements [14], while in this work we did not observe any signs of decomposition of the sample $SrFe_{0.8}Mo_{0.2}O_{3-\delta}$ at 950 °C and oxygen pressure decrease down to $6 \cdot 10^{-18}$ atm, as shown in Fig. 5c.

The p-type electron carriers dominate electron conductivity in the high-pressure range. The conductivity increase with oxygen pressure reflects respective increase in concentration of holes that appear in the oxide in response to oxygen incorporation

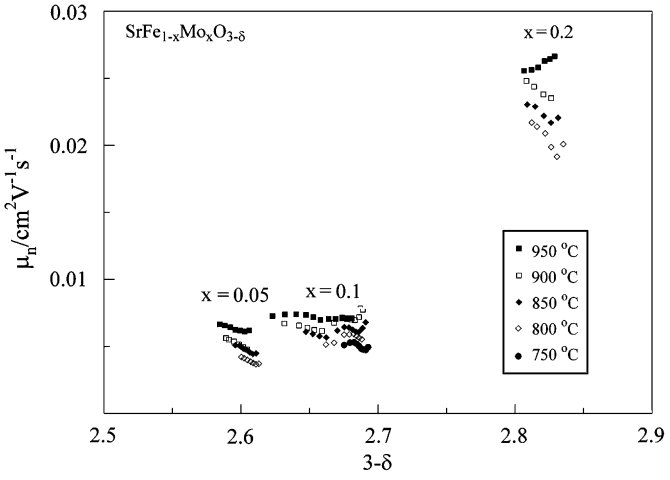

Fig. 8. The mobility isotherms of n-type electron charge carriers in $SrFe_{1-x}Mo_xO_{3-\delta}$ vs. oxygen content.

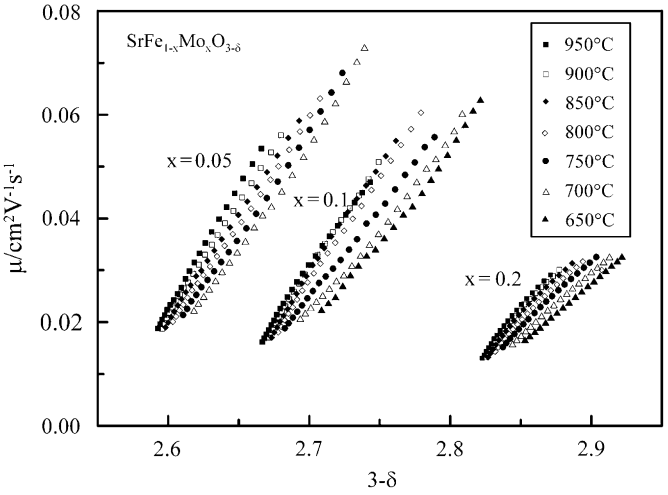

Fig. 10. The mobility isotherms of p-type electron charge carriers in $SrFe_{1-x}Mo_xO_{3-\delta}$ vs. oxygen content.

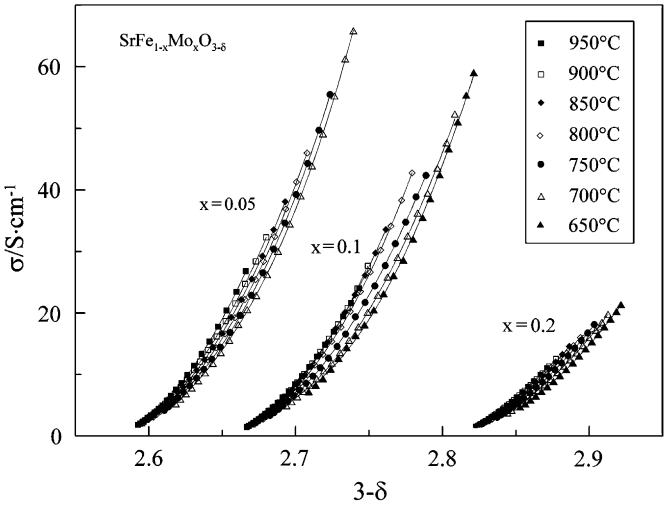

Fig. 9. The isotherms of p-type electron conductivity in $SrFe_{1-x}Mo_xO_{3-\delta}$ depending on oxygen content.

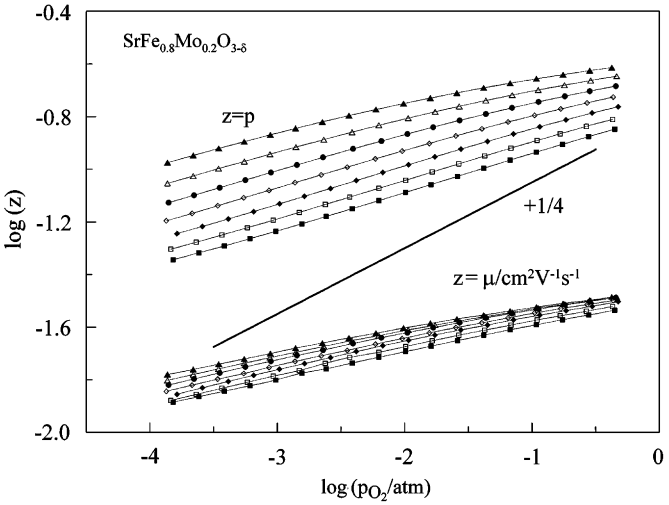

Fig. 11. The isotherms of concentration and mobility of p-type electron charge carriers in $SrFe_{1-x}Mo_xO_{3-\delta}$ vs. partial pressure of oxygen.

reaction (1). The temperature dependence of p-type conductivity at permanent values of oxygen pressure seems to be of a metallic type. However, it is not quite so. Based on the using of pO_2–T–δ interrelations in Fig. 1 we can plot temperature dependencies of hole conductivity at fixed values of oxygen content, i.e. at permanent composition, as shown in Fig. 9. The temperature activated conductivity becomes clearly seen now. The mobility values of p-type carriers as calculated from combined conductivity and oxygen content data are shown in Fig. 10. One can observe that filling of oxygen vacancies with oxygen incorporation results in approximately linear increase in mobility values. This behavior possibly reflects a combined effect of the increase in the amount of transport chains …Fe–O–Fe…, lattice contraction and enhanced overlap of metal-oxygen electron states. The replacement of iron for molybdenum is less unambiguous. On one hand, molybdenum cations are in stable high oxidation state 6+ in the doped ferrite at oxidative conditions, and, therefore, they cannot take direct part in electron transport. Rather, molybdenum substitutions cause damage to the regular order on B-sublattice and, thus, favor decreased mobility of holes. On the other hand, molybdenum doping promotes oxygen vacancy filling that is favorable for the mobility increase. The total effect seems to depend on dopant content. For instance, the substituted sample with $x = 0.05$ reveals mobility level about 30% larger than the parent ferrite [14], and though further doping results in some decrease of the hole mobility it occurs substantially less pronounced than in the case of doping with Ga, Sc or Cr [17,18,29]. On the whole, the calculated migration energy for holes is practically independent on molybdenum content, Table 1.

In the end, we would like to attract attention to the fact that the pressure dependence of isothermal conductivity is sometimes used in order to justify the mechanism of disordering. Heed should be taken here because in essentially nonstoichiometric oxides not only concentration depends on oxygen pressure but mobility of charge carries may also reveal strong pressure dependence. For instance, the slope of the conductivity isotherms in Fig. 5 equals $+\frac{1}{4}$ almost perfectly well. However, it can be seen in Fig. 11, where the data for $SrFe_{0.8}Mo_{0.2}O_{3-\delta}$ are shown as an example, that this slope is a combined result of pressure changes in both concentration and mobility. The pressure exponents $\pm\frac{1}{4}$ can be observed only in the vicinity of intrinsic electron-hole

equilibrium when changes in oxygen content with pressure can be neglected compared to the total content of oxygen in the oxide. Otherwise, oxygen pressure changes may produce more complicated functional dependence of oxygen stoichiometry and, consequently, of conductivity.

4. Conclusion

Structural features, oxygen nonstoichiometry and thermodynamics, oxygen ion and electron transport characteristics are studied in the strontium ferrite doped with molybdenum, $SrFe_{1-x}Mo_xO_{3-\delta}$. The room temperature structure in oxygen depleted samples is shown to change with x from long-range vacancy ordered brownmillerite in the parent ferrite to locally ordered nano-sized vacancy domains in the sample with $x = 0.05$ to the quasi-perovskite cubic structure with approximately random vacancies at $x > 0.1$. The thermodynamics data evidence strong vacancy disordering at heating in more heavily doped samples. It is shown that the bonding energy of the labile oxygen in the crystal lattice tends to decrease with increase in molybdenum content. At the same time, the doping does not make considerable impact upon thermodynamic stability. It is shown that the doping level $x = 0.05$ results in the ion conductivity larger than in the parent ferrite. This change is explained as reflecting the oxygen ion mobility increase in response to the formation of favorable nano-structure in the doped sample. Another important effect of the doping is the electron mobility increase that seems to arise from changes in oxidation state of molybdenum. The combination of thermodynamic and structural stability with enhanced oxygen ion and electron transport parameters attracts attention to the molybdenum doped strontium ferrites, particularly with the doping level near $x = 0.05$, as promising candidate materials for high temperature oxygen separating membranes and SOFC anodes.

Acknowledgments

This work is carried out under partial funding from Russian Foundation for Basic Research (Grants 06-03-33099 and 05-03-08109). Authors are grateful also to the Presidium of the Ural Branch of Russian Academy for the support under Contract no. 7-1K.

References

[1] Y. Teraoka, H.M. Zhang, S. Furukawa, N. Yamazoe, Chem. Lett. 7 (1988) 1084.
[2] A. Holt, T. Norby, R. Glenne, Ionics 5 (1999) 434.
[3] B.C.H. Steele, Solid State Ionics 75 (1995) 157.
[4] H.J.M. Bouwmeester, A.J. Burggraaf, in: A.J. Burggraaf, L. Cot (Eds.), Fundamentals of Inorganic Membrane Science and Technology, Elsevier, Amsterdam, 1996, p. 435.
[5] M. Weston, I.S. Metcalfe, Solid State Ionics 113–115 (1998) 247.
[6] P.N. Dyer, R.E. Richards, S.L. Russek, D.M. Taylor, Solid State Ionics 134 (2000) 21.
[7] J.P. Hodges, S. Short, J.D. Jorgensen, X. Xiong, S.M. Dabrowski, S.M. Mini, C.W. Kimball, J. Solid State Chem. 151 (2000) 190.
[8] M. Schmidt, S.J. Campbell, J. Solid State Chem. 156 (2000) 292.
[9] J.C. Grenier, J. Darriet, M. Pouchard, P. Hagenmuller, Mater. Res. Bull. 11 (1976) 1219.
[10] M.A. Alario-Franco, J.M. Gonzalez-Calbet, M. Vallet, M. Vallet-Regi, J.C. Grenier, J. Solid State Chem. 49 (1983) 219.
[11] J.M. Gonzalez-Calbet, M. Vallet-Regi, M.A. Alario-Franco, J. Solid State Chem. 60 (1985) 320.
[12] J.M. Gonzalez-Calbet, J.M. Alonso, M. Vallet-Regi, J. Solid State Chem. 71 (1987) 331.
[13] A. Nemudry, N. Uvarov, Solid State Ionics 177 (2006) 2491.
[14] M.V. Patrakeev, I.A. Leonidov, V.L. Kozhevnikov, V.V. Kharton, Solid State Sci. 6 (2004) 907.
[15] V.V. Kharton, A.P. Viskup, A.V. Kovalevsky, J.R. Jurado, E.N. Naumovich, A.A. Vecher, J.R. Frade, Solid State Ionics 133 (2000) 57.
[16] J.C. Waerenborgh, D.P. Rojas, A.L. Shaula, G.C. Mather, M.V. Patrakeev, V.V. Kharton, J.R. Frade, Mater. Lett. 59 (2005) 1644.
[17] M.V. Patrakeev, V.V. Kharton, Yu.A. Bakhteeva, A.L. Shaula, I.A. Leonidov, V.L. Kozhevnikov, E.N. Naumovich, A.A. Yaremchenko, F.M.B. Marques, Solid State Sci. 8 (2006) 476.
[18] M.V. Patrakeev, A.A. Markov, I.A. Leonidov, V.L. Kozhevnikov, V.V. Kharton, Solid State Ionics 177 (2006) 1757.
[19] O.A. Savinskaya, A.P. Nemudry, N.Z. Lyakhov, Inorg. Mater. 43 (2007) 1350.
[20] A.A. Markov, I.A. Leonidov, M.V. Patrakeev, V.L. Kozhevnikov, O.A. Savinskaya, U.V. Ancharova, A.P. Nemudry, Solid State Ionics 179 (2008) 1050.
[21] I.A. Leonidov, V.L. Kozhevnikov, E.B. Mitberg, M.V. Patrakeev, V.V. Kharton, F.M.B. Marques, J. Mater. Chem. 11 (2001) 1201.
[22] M.V. Patrakeev, E.B. Mitberg, A.A. Lakhtin, I.A. Leonidov, V.L. Kozhevnikov, K.R. Poeppelmeier, Ionics 4 (1998) 191.
[23] M.V. Patrakeev, J.A. Shilova, E.B. Mitberg, A.A. Lakhtin, I.A. Leonidov, V.L. Kozhevnikov, in: C. Julien, J.P. Pereira-Ramos, A. Momchilov (Eds.), New Trends in Intercalation Compounds for Energy Storage, Kluwer Academic, Dordrecht, 2002, p. 565.
[24] N. Nakayama, M. Takano, S. Inamura, N. Nakanishi, K. Kosuge, J. Solid State Chem. 71 (1987) 403.
[25] M.V. Patrakeev, J.A. Bahteeva, E.B. Mitberg, I.A. Leonidov, V.L. Kozhevnikov, K.R. Poeppelmeier, J. Solid State Chem. 172 (2003) 219.
[26] F.A. Kröger, The Chemistry of Imperfect Crystals, North Holland Publishing Co., Amsterdam, 1964.
[27] J.B. Goodenough, A. Manthiram, P. Paranthaman, Y.S. Zhen, Solid State Ionics 52 (1992) 105.
[28] Y. Tomioca, T. Okuda, Y. Okimoto, R. Kumai, K.I. Kobayashi, Y. Tokura, Phys. Rev. B 61 (2000) 422.
[29] M.V. Patrakeev, I.A. Leonidov, V.L. Kozhevnikov, V.V. Kharton, Mater. Sci. Forum 514–516 (2006) 382.